BUDAPEST UNIVERSITY OF TECHNOLOGY AND ECONOMICS
FACULTY OF CHEMICAL TECHNOLOGY AND BIOTECHNOLOGY
GEORGE A. OLAH DOCTORAL SCHOOL

Influence of Environmental Inhomogeneities on the Optical Scattering Properties of Gold Nanorods

Theses

Author:
Dániel Péter Szekrényes

Supervisor:
Dr. András Deák, senior research fellow (EK MFA)

Internal consultant:
Dr. Zoltán Hórvölgyi, full professor (BME VBK FKAT)

Laboratory of Chemical Nanostructures
Institute of Technical Physics and Materials Science
Centre for Energy Research

2021

1 Introduction

Noble metal nanoparticles show unique optical properties owing to localised surface plasmon resonance that is mainly determined by the geometry of the particles and the dielectric properties of the surrounding medium. At the resonance wavelength they have a large absorption and scattering cross-section, behaving like a lossy nanoantenna, making them an excellent nanoscale heat and scattering source. Gold nanorods support two dipolar plasmon modes associated with the charge oscillation of free electrons along the short and long axes of the elongated particle (transversal and longitudinal plasmon modes). The resonance peak of the longitudinal plasmon mode, which is highly dependent on the aspect ratio of the particle, can be tuned in a wide frequency range via wet-chemical synthesis procedures. Any change in the optical density of near-field of the particle (e.g. because of the surface modification of the particles) leads to changes of the optical scattering spectrum.[1,2] The surface modification of gold nanoparticles plays a key role in practical applications due to the cytotoxic nature of the original CTA^+ capping layer (inherently present after the synthesis).[3,4] One possible way to replace CTA^+ from the particle surface is to use thiol molecules for the ligand exchange due to the strong sulphur-gold interaction.[5]

As a result of environmental inhomogeneities around the nanorods, rich plasmonic phenomena might arise, even when these inhomogeneities are much smaller than the particle size itself. The deeper understanding of the formation and impact of these inhomogeneities and the control over the procedure are, thus, of central importance for diverse applications as well as fundamental research. They provide the possibility to tailor the optical and colloidal properties of the nanoparticles and they enable investigating the impact of the nature (surface chemical or structural) as well as of the extent of the inhomogeneity on the optical properties. A variety of strategies exist to produce environmental inhomogeneities in the vicinity of nanorods. For instance, surface chemical patch can be formed on the particle surface by replacing the original surface layer *via* controlled ligand exchange. The patchy nanorods hold a great potential as building block for self-assembly due to the control over the directionality of colloidal interactions.[6] One can also create environmental inhomogeneity in the optical near-field region of the rod, when the particle is placed onto a nanopatterned substrate with dielectric properties varying on the nanoscale, separated by well-defined boundaries. Furthermore, the presence of another particle in the close proximity of the nanorod can also be considered as the inhomogeneity of the local dielectric environment. For plasmonic nanoparticles, it leads to the modification of the scattering spectrum due to plasmon coupling

[1] Huanjun Chen et al., "Gold Nanorods and Their Plasmonic Properties," *Chem. Soc. Rev.* 42, no. 7 (2013): 2679–2724, https://doi.org/10.1039/C2CS35367A.

[2] Xiaohua Huang, Svetlana Neretina, and Mostafa A. El-Sayed, "Gold Nanorods: From Synthesis and Properties to Biological and Biomedical Applications," *Advanced Materials* 21, no. 48 (December 28, 2009): 4880–4910, https://doi.org/10.1002/adma.200802789.

[3] A. Swarnapali D. S. Indrasekara, Robert C. Wadams, and Laura Fabris, "Ligand Exchange on Gold Nanorods: Going Back to the Future," *Particle & Particle Systems Characterization* 31, no. 8 (August 2014): 819–38, https://doi.org/10.1002/ppsc.201400006.

[4] Nathan D. Burrows et al., "Surface Chemistry of Gold Nanorods," *Langmuir* 32, no. 39 (October 4, 2016): 9905–21, https://doi.org/10.1021/acs.langmuir.6b02706.

[5] Evangelina Pensa et al., "The Chemistry of the Sulfur–Gold Interface: In Search of a Unified Model," *Accounts of Chemical Research* 45, no. 8 (August 21, 2012): 1183–92, https://doi.org/10.1021/ar200260p.

[6] Lubin Zhong et al., "Rational Design and SERS Properties of Side-by-Side, End-to-End and End-to-Side Assemblies of Au Nanorods," *Journal of Materials Chemistry* 21, no. 38 (2011): 14448, https://doi.org/10.1039/c1jm11193k.

and Fano interference. The resulting optical response of the heterodimers are very sensitive to the relative geometrical arrangement of the particles. [7,8,9,10]

2 Aims

In my dissertation, my main objective is to investigate the influence of different inhomogeneous structural changes (surface chemical patch, presence of nanopatterned supporting substrate, heterodimer formation) on the optical properties of plasmonic nanoparticles.

I. One of my goals was to produce and investigate patchy gold nanorods both at the ensemble and single particle levels. The side region of the rod is coated by a neutral polymer called 5 kDa mPEG-SH, while the tips are covered by the much smaller thiol, cysteamine. By using ensemble optical measurements, the relevant ligand concentration range for the ligand exchange can be determined, while relying on single particle experiments, one can get a better understanding of the process. In addition to single particle scattering experiments, correlated scanning probe measurements (scanning electron microscopy, atomic force microscopy) can provide supporting information on the ligand exchange, as these methods can visualise the geometry of the selected patchy nanorods and the morphology of their surface layers (Figure 1).

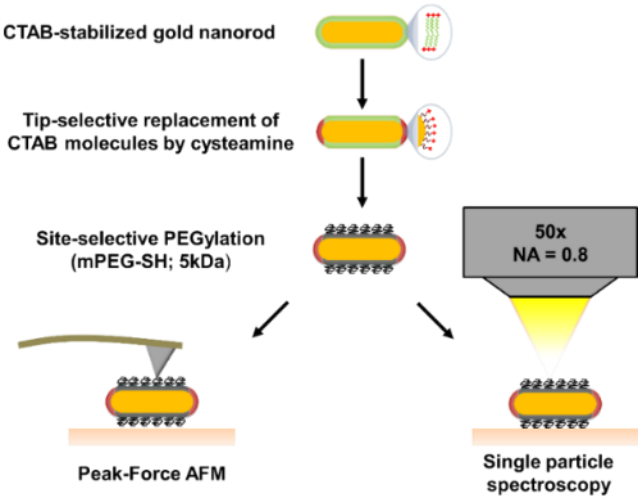

Figure 1. The concept of the preparation of patchy gold nanorods and the investigation of the surface chemical inhomogeneity by using single particle scattering spectroscopy and atomic force microscopy (AFM).

II. Another aim was to investigate the binding of two similar sized, but oppositely charged small-chain thiols (namely cysteamine and 3-mercatopropionic acid (MPA)) on gold nanorods. Under the experimental conditions, cysteamine is positively, while MPA is negatively charged. Besides ensemble optical and electrokinetic measurements, *in-situ* single particle scattering spectroscopy are also carried out in order to overcome the issue of inhomogeneous line broadening of the plasmon peak and the aggregation of the particles. By investigating the resonance wavelength and the plasmon line width of individual gold nanorods, one can gain deeper insight into the accumulation of the two differently charged thiols on the particle surface and the binding process. The single particle experiments are also carried out at different bulk

[7] Peter Zijlstra et al., "Chemical Interface Damping in Single Gold Nanorods and Its Near Elimination by Tip-Specific Functionalization," *Angewandte Chemie International Edition* 51, no. 33 (August 13, 2012): 8352–55, https://doi.org/10.1002/anie.201202318.

[8] Indrasekara, Wadams, and Fabris, "Ligand Exchange on Gold Nanorods."

[9] Huanjun Chen et al., "Effect of the Dielectric Properties of Substrates on the Scattering Patterns of Gold Nanorods," *ACS Nano* 5, no. 6 (June 28, 2011): 4865–77, https://doi.org/10.1021/nn200951c.

[10] Boris Luk'yanchuk et al., "The Fano Resonance in Plasmonic Nanostructures and Metamaterials," *Nature Materials* 9, no. 9 (September 2010): 707–15, https://doi.org/10.1038/nmat2810.

CTAB concentrations to investigate whether there is any interaction between the given thiol molecule and the native surface layer (Figure 2).

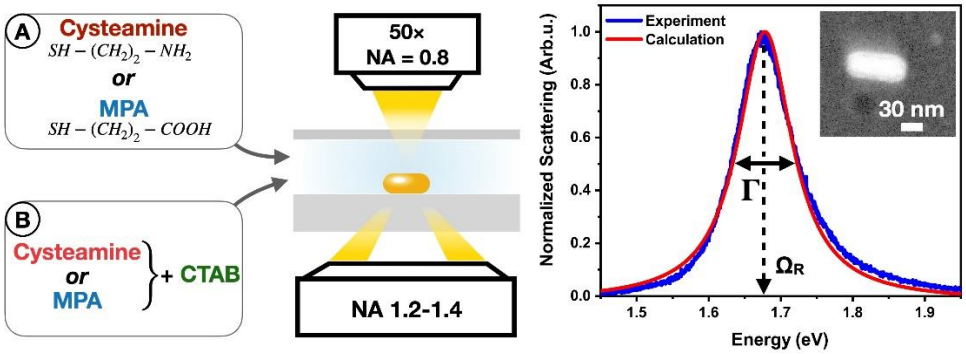

Figure 2. In-situ investigation of the binding of similarly sized, but oppositely charged small-chain thiol ligands via single particle scattering spectroscopy. Besides resonance frequency, plasmon line broadening gives us detailed information on the ligand replacement process.

III. By combining silica nanosphere lithography with Xe^+ ion bombardment, nanopatterned indium tin oxide (ITO) substrates can be produced, having different surface regions (implanted and masked by silica particles) that feature different dielectric functions. The irradiated and non-irradiated regions are separated by sharp boundaries.[11] In my work, gold nanorods placed onto these boundaries, resulting in an environmental inhomogeneity in the close proximity of the rods, leading to the modification of the optical scattering properties of the particle. My goal was to investigate how the extent of the irradiated region below the nanorod and their relative geometrical arrangement influence the optical response of the particles (resonance energy, plasmon line width). In my work, two different configurations are distinguished: one of them is the symmetric bridging configuration, where the tips can be found on the two adjacent unirradiated regions and the centre of the rod is on the implanted area. The other is the overlapping are, where one tip of the rod is located on the masked, while the other tip is on neighbouring irradiated region (Figure 3).

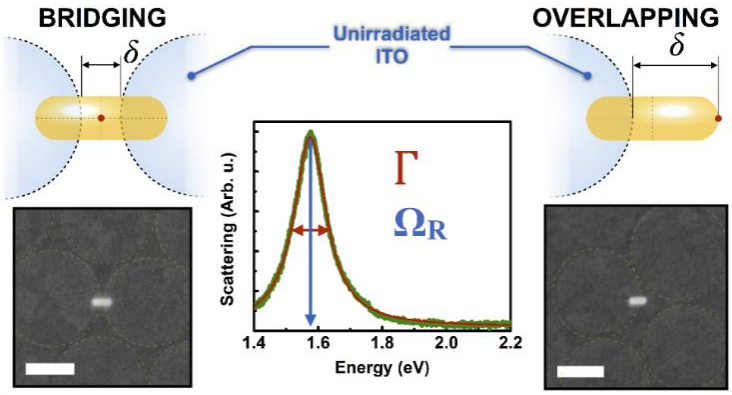

Figure 3.Investigation of the effect of the nanopatterned substrate on the optical properties of individual gold nanorods. In this study, two different configurations are distinguished, namely the bridging and overlapping configurations.

IV. By means of the controlled surface modification of nanoparticles, directed self-assembly can be achieved; by precisely tailoring the colloid interactions sphere/rod heterodimers can be

[11] N. Nagy et al., "Tunable Ion-Swelling for Nanopatterning of Macroscopic Surfaces: The Role of Proximity Effects," *Applied Surface Science* 259 (October 2012): 331–37, https://doi.org/10.1016/j.apsusc.2012.07.045.

prepared in a well-designed way.[12,13] Heterodimers support various coupled plasmon modes that are strongly depends on the geometry of the assembled particle structure.[14] One of my goals was to examine the optical response of the developed heterodimers at the single particle level by using polarisation-resolved single particle scattering spectroscopy and correlative scanning electron microscopy and to establish a connection between the scattering spectrum and the evolved particle structure (Figure 4). In this study, two main heterodimer arrangements were investigated: one of them is when the sphere is located at the top of the nanorod (top-arrangement) and the other is when the sphere can be found at the substrate level adjacent to the rod (side-arrangement). *In-situ* polarisation-resolved single particle measurements enable the more accurate determination of the relative geometrical arrangement in aqueous medium shortly after the self-assembly process.

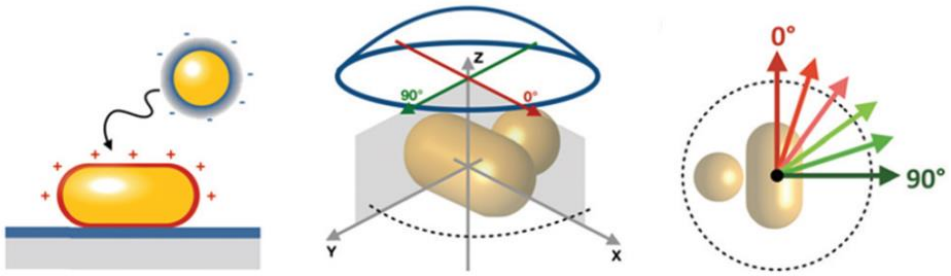

Figure 4. Investigation of the relative geometrical rearrangement of gold rod/sphere heterodimers developed via electric double layer directed self-assembly procedure. To determine the evolved structure in situ polarization resolved scattering spectroscopy is carried out.

3 Methods

Gold nanoparticles used in this study were prepared by using wet-chemical syntheses procedures. Citrate-stabilised spherical gold nanoparticles with the diameter of 50 nm synthesised based on the seeded-growth procedure published by *Ziegler et al*.[15] Gold nanorods with different dimensions were produced by carefully adjusting the synthesis conditions and controlling the amount of additives.[16] The extinction spectra of the as-synthetized gold nanoparticles is shown in Figure 5.

[12] S. Pothorszky et al., "Detecting Patchy Nanoparticle Assembly at the Single-Particle Level," *Nanoscale* 9, no. 29 (2017): 10344–49, https://doi.org/10.1039/C7NR02623D.

[13] Sz. Pothorszky et al., "Assembling Patchy Nanorods with Spheres: Limitations Imposed by Colloidal Interactions," *Nanoscale* 8, no. 6 (2016): 3523–29, https://doi.org/10.1039/C5NR08014B.

[14] Lei Shao et al., "Distinct Plasmonic Manifestation on Gold Nanorods Induced by the Spatial Perturbation of Small Gold Nanospheres," *Nano Letters* 12, no. 3 (March 14, 2012): 1424–30, https://doi.org/10.1021/nl2041063.

[15] Christoph Ziegler and Alexander Eychmüller, "Seeded Growth Synthesis of Uniform Gold Nanoparticles with Diameters of 15−300 Nm," *The Journal of Physical Chemistry C* 115, no. 11 (March 24, 2011): 4502–6, https://doi.org/10.1021/jp1106982.

[16] Xingchen Ye et al., "Using Binary Surfactant Mixtures To Simultaneously Improve the Dimensional Tunability and Monodispersity in the Seeded Growth of Gold Nanorods," *Nano Letters* 13, no. 2 (February 13, 2013): 765–71, https://doi.org/10.1021/nl304478h.

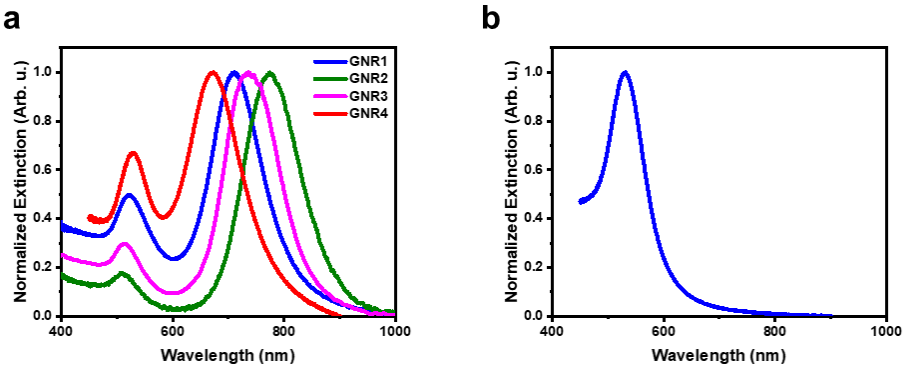

Figure 5 The ensemble optical spectra of gold nanorods (a) and nanospheres (b) used in this work.

The original CTAB bilayer of the nanorods formed during the synthesis were replaced through a ligand exchange process using thiol molecules. To do this, the solution of the thiol ligand at given concentration were added to the CTAB-stabilised gold nanorods. After the surface modification procedure, the solutions were centrifuged and washed to remove the excess, unreacted thiol molecules from the aqueous phase. The modification and purification process were monitored by utilising a fibre-coupled diode-array visible spectrometer (Thorlabs CCS200) and electrophoretic mobility measurements (Malvern Zetasizer NanoZS).

Samples for studying the influence of surface chemical patch formation and substrate inhomogeneities at the single particle level were prepared by spin-coating technique. Using a dark-field optical microscope (Olympus BX51) in epi-illumination mode, individual particles were selected and their scattering spectra were obtained using a microscope coupled, aberration-corrected imaging spectrograph (Princeton Instruments Isoplane SCT320) that is equipped with a high sensitivity, cooled CCD detector (Princeton Instruments PIXIS:400BRX). For the precise control over the sample and particle positions, an XYZ piezo stage (Physik Instrumente, P-545.3R8S) was used. After the single particle optical experiments, the very same nanorods were measured by scanning probe experiments (scanning electron microscopy, atomic force microscopy).

For single particle experiments in aqueous medium, a liquid cell was assembled with the spin-coated particles on the bottom plate. In this case, the optical upright microscope was used in trans-illumination mode. The liquid cell (HybriWell HBW6021-GraceBiolabs) was mounted on the microscope stage of the upright optical microscope equipped with a dedicated oil-immersion dark-field condenser (Olympus U-DCW, NA = 1.2−1.4). After the integration of the liquid cell into the microscope, the rods were conditioned with different short-chain thiol solutions from 10^{-4} to 10^{2} mM ligand concentrations for 20 minutes after which the scattering spectra of the same nanorods were acquired. The same procedure was performed at different background CTAB concentrations.

The heterodimer formation was carried out in another type of liquid cell. In this case, the surface modified nanorods were spin-coated on a cleaned ITO-coated glass substrate, which was the bottom plate of the liquid cell, while a glass cover slide was used as top plate. As a spacer, Parafilm was used. Polarisation-resolved spectra of the selected heterodimers were obtained by placing a linear polariser (Thorlabs LPVISC100-MP2) mounted in a motorised rotary stage directly in front of the entrance slit of the imaging spectrometer.

The *ex-situ* SEM images were obtained by using a Zeiss LEO field emission scanning electron microscope operated at the acceleration voltage of 5 kV after disassembling the liquid chamber.

4 Results

4.1 Investigating the patch formation at the tips of gold nanorods

By using a two-step surface modification process gold nanorods with surface chemical inhomogeneity were prepared. The tips of the rods are coated by the small, positively charged cysteamine, while the side region is covered by 5 kDa mPEG-SH. The addition of cysteamine to the particle solution with increasing bulk thiol concentration results in a blueshift in the longitudinal plasmon peak and increasing electrokinetic mobility. The longitudinal plasmon peak position gives information on the local optical density of the near-field region at the tips, while electrokinetic measurements characterise the entire particle surface. Relying the combination of the two ensemble measurements, one can monitor the selective surface modification process. As Figure 6 shows, both the blue shift and electrophoretic mobility reach their final value at 10^{-2} mM cysteamine concentration, indicating the saturation of the tips by cysteamine. These findings are consistent with the earlier results of our research group, [17,18] there is, however a significant difference. My results indicate that when larger nanorods are used, where the CTAB bilayer can be considered as more compact (due to the smaller curvature and better developed particle facets), the binding of cysteamine in more effectively blocked (almost constant blueshift and electrophoretic mobility above the critical concentration).

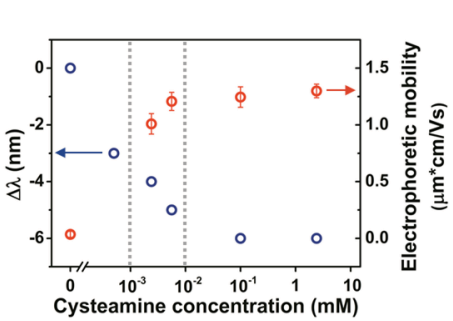

Figure 6. The blueshift of longitudinal plasmon peak and the increase of electrophoretic mobility as a function of cysteamine concentration. Based on the results, the critical cysteamine concentration is 10^{-2} mM.

Correlated SEM micrographs show that the selected particles have a well-defined rod shape and no contamination can be seen in the vicinity of the particles. The correlated AFM deformation maps of nanorods covered by 5 kDa mPEG-SH and MTAB (similarly to cysteamine a rigid thiol) reveal that there is a significant difference in the capping ligand layers. An approximately 5 nm thick, deformable layer can be observed on PEGylated rods, while for MTAB-coated particles, a more rigid and much thinner layer can be seen. Both structural features of the afore-mentioned surface layers can be simultaneously observed for patchy nanorods, that is, where the side region of the rod is covered by the mPEG-SH and a well-defined surface chemical inhomogeneity can be found at the tips. The tendency in the resonance wavelength of the particles are in agreement with the AFM measurements: the PEGylated particle having the highest optical density at the tips has the highest resonance wavelength, while the shortest resonance wavelength is found for the patchy particle, which correlates with the optical density of the rod tip's optical near-field region.

[17] Pothorszky et al., "Detecting Patchy Nanoparticle Assembly at the Single-Particle Level."
[18] Pothorszky et al., "Assembling Patchy Nanorods with Spheres."

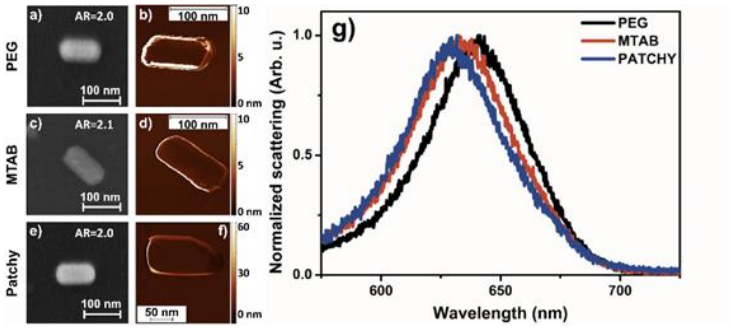

Figure 7.SEM micrographs (a, c, e), AFM deformation maps (b, d, f) and optical scattering spectra (g) of the selected, individual gold nanorods

In the AFM image of a gold nanorod modified at lower cysteamine concentration (10^{-3} mM) no surface chemical patch development can be seen. However, there is a measurable blueshift of longitudinal plasmon resonance peak obtained from ensemble optical experiments, indicating that the binding of cysteamine still takes place at the tips. These findings suggest that this lower cysteamine concentration is not able to form a well-defined patch and the remaining sites were occupied by mPEG-SH. Optical simulations based on finite element method clarify that the homogeneous change in the optical density of the surrounding medium and the inhomogeneous change in the extent of the patch results in similar tendency in terms of the resonance wavelength, which is consistent with the findings obtained from AFM images. As a result, using only optical spectroscopy is insufficient to unambiguously identify the structure of the surface layer.

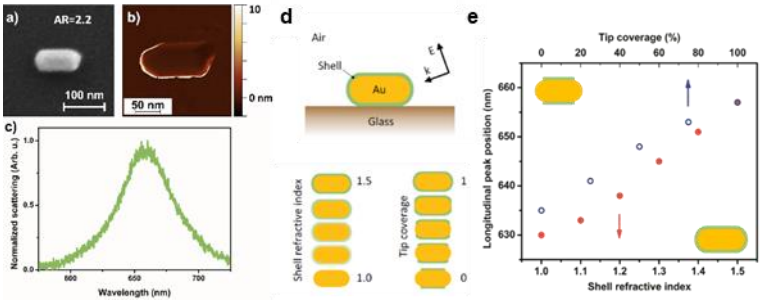

Figure 8. SEM image (a), AFM deformation map (b) and single particle scattering spectrum (c) of a gold nanorod modified at lower cysteamine concentration (10^{-3} mM). Investigating the effect the effective refractive index of the shell and the tip coverage of the patch. (d). Similar trends of longitudinal plasmon wavelength as a function of patch size and the effective refractive index of the shell. (e)

4.2 Investigating the binding of differently charged short-chain thiol-ligands on CTAB-capped gold nanorods by analysing chemical interface damping changes

The binding of differently charged, but similar sized small-chain thiol molecules (cysteamine and 3-mercaptopropionic acid(MPA)) on gold nanorods was investigated relying on optical measurement techniques both at ensemble and single particle levels. Interestingly, regardless the different charge of the two molecules, the ensemble results show that increasing amount of both thiol ligands causes the increase of electrophoretic mobility of the rods. While the addition of cysteamine results in a blueshift of the longitudinal plasmon peak in agreement with the earlier results, the binding of MPA leads to a significant redshift. This effect might be interpreted by the electrostatic interaction between the thiol ligand and the native CTA^+ layer, inducing the accumulation of the CTA^+ molecules around the rods that results in an increase of the optical density of the near-field region.

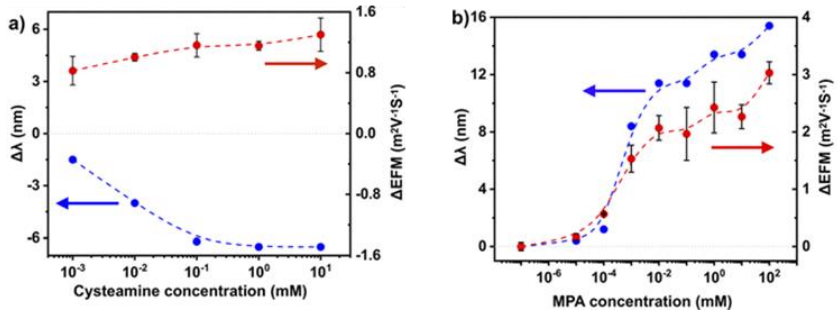

Figure 9. The shift of the longitudinal resonance peak of gold nanorods and the changes in the electrophoretic mobility upon the addition of cysteamine (a) and MPA (b).

To corroborate this mechanism and to rule out the effect of aggregation, the ligand exchange procedure was also studied at the level of individual nanorods. The tendencies of the resonance wavelength and plasmon linewidth demonstrate the reduced binding of MPA compared to cysteamine. While cysteamine can readily replace the CTA^+ molecules from the particle surface, the binding of MPA is more inhibited process due to the interaction between the negatively charged MPA and CTA^+. This already indicates that bound MPA stabilises CTAB at the particles' surface.

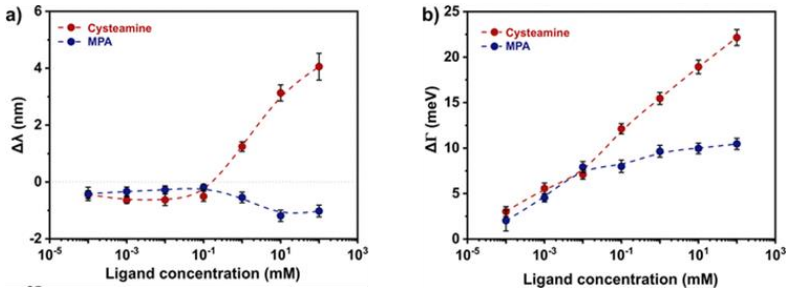

Figure 10. Changes in longitudinal resonance peak position (a) and plasmon line width (b) of individual gold nanorods at different thiol concentrations.

To investigate how this effect scales with the bulk CTAB concentration, the binding of MPA were carried out at different CTAB background concentrations. The results corroborate the previous observations according to which the increasing bulk CTAB concentration leads to a more reduced amount of bound MPA.

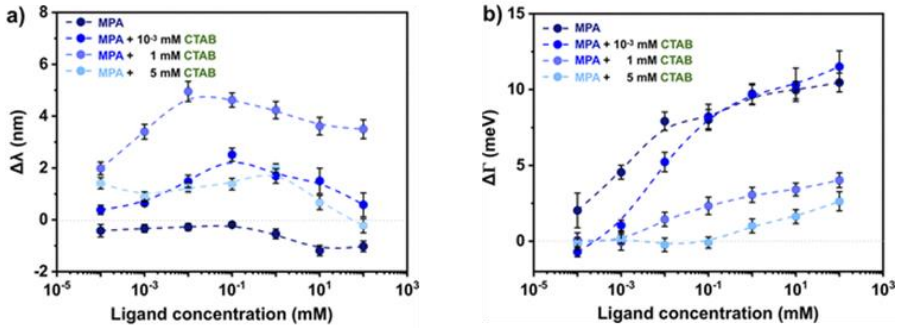

Figure 11. Plasmon peak shift (a) and line width broadening (b) as a result of MPA binding at different bulk CTAB concentrations.

4.3 Gold nanorod plasmon resonance damping effects on a nano-patterned substrate

Changes in the resonance frequency and the plasmon line width of gold nanorods located on a nanopatterned surface were investigated in the framework of the dipole antenna theory as a function of the extent of irradiated region below the particle for two different particle configurations (bridging and overlapping). By analysing these parameters, it was shown that

for bridging configuration the plasmon damping of the gold nanorod gradually increases as a function of the area of the implanted zone. In contrast, an abrupt broadening of the plasmon peak can be detected for overlapping configuration and it reaches its limiting value when the one-third of the rod is located on the irradiated zone. These observations demonstrate that the dielectric and physical-chemical properties of the different regions on the supporting substrate can strongly modify the original optical response of the particle, even if these inhomogeneities are smaller than the particle size itself. The observed differences for the two arrangements might be originating in the local dielectric property dependent induced mirror charges in the substrate.

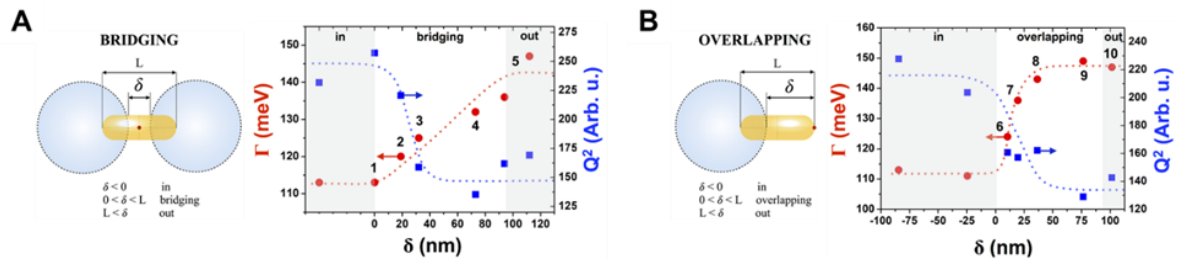

Figure 12. Changes in the plasmon damping and the quality factor as a function of the extent of substrate inhomogeneity for the case of the bridging (a) and overlapping configurations (b).

4.4 Spatial rearrangement of gold nanorod/nanosphere heterodimers and their polarisation-dependent optical response

Gold nanosphere/nanorod heterodimers prepared by tailoring the surface chemical properties of the nanoparticles were investigated by single particle scattering spectroscopy. Based on the white-light scattering spectroscopy experiments, no difference can be observed between the optical responses of the top- and side-arranged heterodimers. To differentiate between these two main arrangements optically, polarisation-resolved scattering spectra were acquired. It derived from optical simulations that the spatial orientation of the coupling axis of the sphere dipolar/rod transversal mode can give information on the relative geometrical arrangement of the particles in case of the polarisation-resolved acquisition of the scattering spectra. For side arrangement, the peak associated with the coupled mode can be detected with analyser angle parallel to the coupling axis, for top arrangement, however, the contribution of this mode becomes negligible because of the perpendicular orientation of the coupling axis.

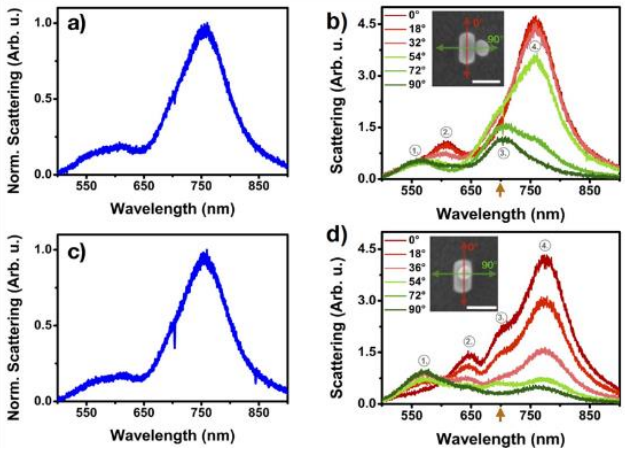

Figure 13. White-light scattering spectra of gold sphere/rod heterodimers with top- and side arrangements. (a, c) Polarisation-resolved scattering spectra of the same heterodimers. (b, d) The different polarization-dependent behaviour of the coupled sphere dipolar/rod transversal mode (indicated with orange arrow) of the two arrangements can provide more information on the relative spatial arrangement of the rod/sphere heterodimers.

These findings can be utilised to *in-situ* determine the developed particle structure upon the electric double layer directed self-assembly procedure in the liquid environment. It was

demonstrated using single particle scattering spectroscopy and correlative SEM measurements, that both the top and side particle arrangements evolve upon heterodimer assembly, and that spheres located at the top of the rod might shift to the substrate level during the drying of the system under the action of immersion type capillary forces.

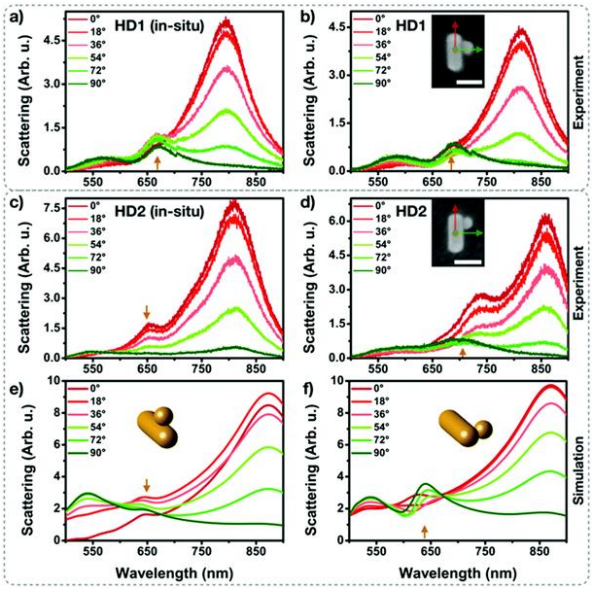

Figure 14. Polarization-resolved scattering spectra measured for two heterodimers (HD1: a and b; HD2: c and d) before (a and c) and after (b and d) structural characterization using SEM. The insets in b and d show the actual arrangement of the heterodimers measured ex-situ. The bottom row (e and f) shows the simulated spectra for HD2 together with the anticipated geometrical arrangements. The orange arrows mark the positions of the sphere dipole-rod transversal coupled modes. Scale bars in SEM insets: 100 nm.

5 List of theses

1. Realising correlative single particle spectroscopy/atomic force microscopy I provided direct experimental evidence for the first time on the development of well-defined surface chemical inhomogeneity at the tips of the investigated gold nanorods (55 × 115 nm) using a two-step surface modification procedure: above 10^{-2} mM cysteamine concentration the tips were covered by cysteamine, while the side region was coated by 5 kDa mPEG-SH. I showed that at lower concentrations no well-defined cysteamine patch evolves even though some ligand exchange still takes place. [T1]

2. By means of optical simulations I showed for the first time that although the scattering spectra of individual gold nanorods is sensitive to the binding of different ligands at the interface, the presence of a well-defined, surface chemical inhomogeneity cannot be concluded solely on the basis of the optical density change related resonance peak shift. This derives from the similar wavelength shift caused by the spatially homogeneous and inhomogeneous refractive index changes at the close proximity of the nanoparticle surface. [T1]

3. I was the first to utilise the chemical interface damping changes determined from the scattering spectrum of individual, CTAB-capped gold nanorods to study the ligand exchange procedure. Based on the measurements performed in 10^{-4}-10^{2} mM thiol ligand (cysteamine, 3-mercaptopropionic acid) concentration range, I demonstrated that there is difference between the adsorption of the positively charged cysteamine and the negatively charged 3-mercaptopropionic acid on CTAB-capped gold nanorods. [T2]

4. By varying the bulk CTAB concentration in 0-5 mM range I showed that the different extent of cysteamine and 3-mercaptopropionic acid binding is a result of the interaction between the differently charged small thiols and CTA^{+} layer: while cysteamine is effectively replacing CTAB, 3-mercaptopropionic acid stabilises the CTAB at the nanorods' surface, hence its accumulation at the particle interface is lower compared to cysteamine. [T2]

5. I investigated for the first time how inhomogeneities of the local substrate dielectric properties influence on the scattering spectrum of the substrate-attached gold nanorods. The plasmon line width of the particles located on sharp, well-defined boundaries of an ion implanted substrate depends differently on the extent of inhomogeneity for the symmetric and asymmetric cases: for the rods, experiencing symmetric inhomogeneity, plasmon line width varies proportionally with the extent of inhomogeneity. For asymmetric case, a more abrupt increase of the damping was found, already when one third of the nanorod is located over the irradiated region, the damping reaches its limiting value. I assigned the induced mirror charges in the substrate as the possible origin of this symmetry-dependent behaviour. [T3]

6. I demonstrated for the first time, that polarisation-resolved optical scattering spectrum measurements allow to distinguish between the two main arrangements of gold nanosphere/nanorod heterodimers, that is when the gold nanosphere is located on the top of the gold nanorod or at the substrate level. Based on optical simulations that also account for the given experimental arrangement, I concluded that the difference between the polarisation-dependent optical responses of the two configurations stems from the different spatial orientation of the sphere dipolar/rod transversal coupled mode. [T4]

7. I utilised *in-situ* polarisation-resolved optical scattering microscopy for the first time to investigate which relative particle arrangements develop upon the self-assembly of gold nanospheres and nanorods in aqueous medium. Based on the scattering spectra of the developing individual heterodimers I confirmed that during the process, the nanosphere can attach both to the upper and side region of the solid/liquid interface located nanorod. By using correlative microspectroscopy/electron microscopy I demonstrated that the configuration of the heterodimers can rearrange during the drying procedure as a result of immersion type capillary forces. [T4]

6 Publications

Publications related to the thesis

[T1] **Szekrényes, D. P.**; Pothorszky, S.; Zámbó, D.; Osváth, Z.; Deák, A. Investigation of Patchiness on Tip-Selectively Surface-Modified Gold Nanorods. The Journal of Physical Chemistry C 2018, 122 (3), 1706–1710. https://doi.org/10.1021/acs.jpcc.7b11211.

[T2] **Szekrényes, D. P.;** Kovács, D.; Zolnai, Z.; Deák, A. Chemical Interface Damping as an Indicator for Hexadecyltrimethylammonium Bromide Replacement by Short-Chain Thiols on Gold Nanorods. J. Phys. Chem. C 2020, 124 (36), 19736–19742. https://doi.org/10.1021/acs.jpcc.0c04629

[T3] Zolnai, Z.; Zámbó, D.; Osváth, Z.; Nagy, N.; Fried, M.; Németh, A.; Pothorszky, S.; **Szekrényes, D. P**.; Deák, A. Gold Nanorod Plasmon Resonance Damping Effects on a Nanopatterned Substrate. J. Phys. Chem. C 2018, 122 (43), 24941–24948. https://doi.org/10.1021/acs.jpcc.8b07521.

[T4] **Szekrényes, D. P.;** Pothorszky, S.; Zámbó, D.; Deák, A. Detecting Spatial Rearrangement of Individual Gold Nanoparticle Heterodimers. Phys. Chem. Chem. Phys. 2019, 21 (19), 10146–10151. https://doi.org/10.1039/C9CP01541H.

Other publications

[1] Pothorszky, S.; Zámbó, D.; **Szekrényes, D. P.**; Hajnal, Z.; Deák, A. Detecting Patchy Nanoparticle Assembly at the Single-Particle Level. Nanoscale 2017, 9 (29), 10344–10349. https://doi.org/10.1039/C7NR02623D.

[2] Zámbó, D.; **Szekrényes, D. P.**; Pothorszky, S.; Nagy, N.; Deák, A. SERS Activity of Reporter-Particle-Loaded Single Plasmonic Nanovoids. J. Phys. Chem. C 2018, 122 (41), 23683–23690. https://doi.org/10.1021/acs.jpcc.8b06716.

[3] Albert, E.; Tegze, B.; Hajnal, Z.; Zámbó, D.; **Szekrényes, D. P.**; Deák, A.; Hórvölgyi, Z.; Nagy, N. Robust Contact Angle Determination for Needle-in-Drop Type Measurements. ACS Omega 2019, 4 (19), 18465–18471. https://doi.org/10.1021/acsomega.9b02990.

[4] **Szekrényes, D. P.**. Az arany a nanotechnológia szolgálatában: Trükkös színektől a rákgyógyításig. Élet és Tudomány, 2020, (38), 1196-1198.

Oral presentations

Szekrényes, D. P.; Pothorszky S.; Zámbó D.; Osváth Z.; Deák A. Investigating the self-assembly of molecules and nanoparticles on the surface of individual gold nanorods. *European Student Colloid Conference*, Varna, Bulgaria, 2019

Szekrényes, D. P.; Pothorszky S.; Zámbó D.; Hajnal Z.; Osváth Z., Deák A. Surface chemical patch formation and self-assembly studied at the single-nanoparticle level, *XXV. Nemzetközi Vegyészkonferencia*, Kolozsvár, Románia, 2019

Szekrényes, D. P.; Zámbó, D.; Zolnai, Z.; Nagy, N.; Deák, A. Detecting short-chain thiol binding on CTAB-stabilised gold nanorods at single particle level, Mátraháza, Hungary, 2020

Zolnai, Z.; Zámbó, D.; **Szekrényes, D. P**, Deák, A. Radiative damping of surface plasmon resonance in gold nanoparticles: the effect of shape, size, and substrate material, *E-MRS 2019 Fall Meeting*, Warsaw, 2019

Zámbó, D.; **Szekrényes, D. P.**; Pothorszky, S.; Schlosser, A.; Rusch, P.; Lübkemann, F.; Wang, Y.; Nagy, N.; Deák, A.; Bigall, N. C. Two- and three-dimensional self-assembly of plasmonic and semiconductor nanoparticles: from nanopatterning to self-supported aerogels, *MUPHARM 2019*, Ain Sokhna, Egypt, 2019

Szekrényes, D. P.; Pothorszky, S.; Zámbó, D.; Hajnal, Z.; Osváth, Z.; Deák; A. Patchy nanoparticles and their assemblies investigated at the single particle level, *11th Conference on Colloid Chemistry*, Eger, Hungary, 2018

Szekrényes, D. P.; Pothorszky, S.; Zámbó, D.; Hajnal, Z.; Osváth, Z.; Deák, A. Surface chemical patch formation and self-assembly investigated at the single-particle level, *ECIS 2018*, Ljubljana, Slovenia, 2018

Pothorszky, S.; Zámbó D.; **Szekrényes, D.**; Deák, A. Region-selective self-assembly of patchy particles investigated at the single particle level, *2018 Early Career Scientist Summit*, Physical Laboratory, Teddington, United Kingdom, 2018

Pothorszky, S.; Zámbó D.; **Szekrényes, D. P.**; Hajnal, Z.; Deák, A. Patchy nanoparticle preparation and assembly, *ECIS 2017*, Madrid, Spain, 2017

Poster presentations

Szekrényes, D. P.; Pothorszky, P.; Zámbó, D.; Osváth, Z.; Deák, A. Patch formation on tip-selectively modified gold nanorods at the single particle level, *11th Conference on Colloid Chemistry*, Eger, Hungary, 2018

Szekrényes, D. P.; Pothorszky, S.; Zámbó, D.; Hajnal, Z.; Deák, A. Detecting the spatial arrangement of gold nanoparticle heterostructures at the single particle level *15th Zsigmondy Colloquium*, Dresden, Germany, 2019

Zámbó, D.; **Szekrényes, D. P.**; Pothorszky, S.; Nagy, N.; Deák, A. Reporter-particle loaded single plasmonic nanovoids and their SERS activity *118th General Assembly of the German Bunsen Society for Physical Chemistry*, 2019, Jena, Germany, 2019

Szekrényes, D. P.; Pothorszky, S.; Zámbó, D.; Osváth, Z.; Zolnai, Z.; Deák, A. Nanoscale inhomogeneities characterized by the optical scattering spectra of individual gold nanoparticles, *33rd Conference of the European Colloid and Interface Society*, Leuven, Belgium, 2019

Albert, E.; Tegze, B.; Hajnal, Z.; Zámbó, D.; **Szekrényes, D. P.**; Hórvölgyi, Z.; Nagy, N. Simple and robust contact angle determination for sessile drops without apex, *XXV. Nemzetközi Vegyészkonferencia*, Kolozsvár, Románia, 2019

Zámbó, D.; **Szekrényes, D. P.**; Pothorszky, S.; Nagy, N.; Deák, A. Reporter particle-loaded single plasmonic nanovoids and their SERS activity, *118th General Assembly of the German Bunsen Society for Physical Chemistry*, Jena, Germany, 2019

Zámbó, D.; Pothorszky, S.; Szekrényes, D. P.; Deák, A. Perturbation-induced clustering of PEGylated gold nanoparticles, *11th Conference on Colloid Chemistry*, Eger, Hungary, 2018